

# SOLPS-ITER simulations of a vapour box design for the linear device Magnum-PSI

**Citation for published version (APA):**

Gonzalez, J., Westerhof, E., & Morgan, T. W. (2023). SOLPS-ITER simulations of a vapour box design for the linear device Magnum-PSI. *Plasma Physics and Controlled Fusion*, 65(5), Article 055021.  
<https://doi.org/10.1088/1361-6587/acc8fa>

**Document license:**

TAVERNE

**DOI:**

[10.1088/1361-6587/acc8fa](https://doi.org/10.1088/1361-6587/acc8fa)

**Document status and date:**

Published: 01/05/2023

**Document Version:**

Publisher's PDF, also known as Version of Record (includes final page, issue and volume numbers)

**Please check the document version of this publication:**

- A submitted manuscript is the version of the article upon submission and before peer-review. There can be important differences between the submitted version and the official published version of record. People interested in the research are advised to contact the author for the final version of the publication, or visit the DOI to the publisher's website.
- The final author version and the galley proof are versions of the publication after peer review.
- The final published version features the final layout of the paper including the volume, issue and page numbers.

[Link to publication](#)

**General rights**

Copyright and moral rights for the publications made accessible in the public portal are retained by the authors and/or other copyright owners and it is a condition of accessing publications that users recognise and abide by the legal requirements associated with these rights.

- Users may download and print one copy of any publication from the public portal for the purpose of private study or research.
- You may not further distribute the material or use it for any profit-making activity or commercial gain
- You may freely distribute the URL identifying the publication in the public portal.

If the publication is distributed under the terms of Article 25fa of the Dutch Copyright Act, indicated by the "Taverne" license above, please follow below link for the End User Agreement:

[www.tue.nl/taverne](http://www.tue.nl/taverne)

**Take down policy**

If you believe that this document breaches copyright please contact us at:

[openaccess@tue.nl](mailto:openaccess@tue.nl)

providing details and we will investigate your claim.

PAPER

## SOLPS-ITER simulations of a vapour box design for the linear device Magnum-PSI

To cite this article: J Gonzalez *et al* 2023 *Plasma Phys. Control. Fusion* **65** 055021

View the [article online](#) for updates and enhancements.

### You may also like

- [A simplified lithium vapor box divertor](#)  
E.D. Emdee, R.J. Goldston, J.A. Schwartz et al.
- [The effect of gas injection location on a lithium vapor box divertor in NSTX-U](#)  
E.D. Emdee and R.J. Goldston
- [Self-consistent modelling of a liquid metal box-type divertor with application to the divertor tokamak test facility: Li versus Sn](#)  
G.F. Nallo, G. Mazzitelli, L. Savoldi et al.

# SOLPS-ITER simulations of a vapour box design for the linear device Magnum-PSI

J Gonzalez<sup>1,\*</sup> , E Westerhof<sup>1</sup>  and T W Morgan<sup>1,2</sup> 

<sup>1</sup> DIFFER, de Zaale 20, 5612AJ Eindhoven, The Netherlands

<sup>2</sup> Department of Applied Physics, Eindhoven University of Technology, Groene Loper 19, 5612 AP Eindhoven, The Netherlands

E-mail: [j.gonzalezmunos@diffen.nl](mailto:j.gonzalezmunos@diffen.nl)

Received 6 November 2022, revised 15 March 2023

Accepted for publication 30 March 2023

Published 11 April 2023



CrossMark

## Abstract

A vapour box (VB) is a physical device currently being considered to reduce the high heat and particle fluxes typically impacting the divertor in tokamaks. This system usually consists of a series of boxes that retains neutral particles to increase the amount of collision events with the impacting plasma. The neutral particles come from recycling and recombination of the plasma, gas puffing inside the box and by the evaporation of a liquid metal, typically Li or Sn. Currently, an VB is being constructed for testing in the linear plasma generator Magnum-PSI, operated at DIFFER. Its modular design will allow for open (not enclosing the target) and closed (enclosing the target) configurations, as well as evaporating a liquid metal to create a vapour cloud inside the box. The experiments carried out with this device will investigate its capabilities to reduce the plasma flux towards the target. This work presents a numerical study performed with SOLPS-ITER about the effectiveness of the current VB design in its open configuration to retain neutrals and its effect on the plasma beam properties. This is a first step before validation against experiments and studying closed configurations to ensure that the VB can successfully operate in a wide range of plasma parameters. Simulations show that the VB is capable of retaining neutrals and reducing fluxes to the target without requiring additional gas puffing in High and Low plasma flux scenarios. When lithium is evaporated from inside the box, the hydrogen plasma is completely extinguished and replaced by a low temperature Li plasma with lower flux. The fraction of Li and Li<sup>+</sup> transported upstream the VB is three orders of magnitude below the amount evaporated from the central box, as most of the lithium is condensed in the side boxes and another small portion (two orders of magnitude below the amount evaporated) is deposited on the target. The VB design in its open configuration can mitigate incoming plasma peak heat flux by 0.6 MW m<sup>-2</sup>, which represents a fraction of 75% and 81% for the High and Low flux scenarios. This effect is expected to be higher when a closed configuration is employed, which could result in a significant reduction of heat fluxes on the divertor of tokamaks once that this design is extrapolated to the toroidal geometry, with just a minimal amount of Li and Li<sup>+</sup> reaching the core.

Keywords: SOLPS, simulations, vapour box, liquid divertors

(Some figures may appear in colour only in the online journal)

\* Author to whom any correspondence should be addressed.

## 1. Introduction

Control of power exhaust in a tokamak's divertor is a key element for the next generation of power plants [1–3]. The amount of heat that the divertor is capable of sustaining will constrain the operation of reactors and the production of energy. Thus, controlling and reducing the heat fluxes sustained by the divertor is key for fusion devices like ITER and DEMO. Moreover, the reduction of heat and particle fluxes will extend the lifetime of the divertor by reducing erosion and other possible sources of damage and defects. The method employed must ensure a low contamination of the plasma core, i.e. the upstream flow of impurities should be minimised. Multiple techniques are being considered for this function such as gas puffing [4–7] or liquid divertors [8, 9]. Because the evaporated gases of liquid metals easily condense on solid surfaces, the flux of particles to the core can be strongly reduced by strong baffling and the re-condensation and re-circulation of liquid metals. This can be achieved by making a strongly closed divertor with up to several separate chambers with narrow openings for the scrape-off layer plasma to pass through. This vapour box (VB) approach [10–12] shows promise in modelling, but it is not yet experimentally verified in a plasma loading scenario.

A modular concept for an VB test module is currently being designed at DIFFER to be tested in the linear plasma device Magnum-PSI [12, 13]. Multiple configurations of the box and plasma scenarios will be studied to characterize the capabilities of this VB to mitigate the plasma beam. These include an open scenario where the plasma beam passes through each box and emerges before impacting the target, and a closed scenario where the target is surrounded by the final box. A general scheme of Magnum-PSI with the open configuration of the VB can be found in figure 1.

This work presents simulations performed with the edge plasma code SOLPS-ITER [14] to study the performance of the VB module in different Magnum-PSI plasma scenarios. The capability of the VB to retain neutrals coming from plasma recombination and target recycling as well as the evaporation of a liquid metal, lithium, in the open configuration are presented. This open configuration allows for the easy measurement of plasma properties in the region after the interaction with the neutrals contained by the box, especially by Thomson Scattering (TS), which is necessary to characterise the VB and for the future validation of these simulations. Once simulations are compared with experimental data and the model produces comparable results to the experiment, the closed configuration will be simulated to properly study the capability of this VB to mitigate the plasma flow.

This paper is organised as follows. Section 2 presents a simple introduction to the linear device simulated, Magnum-PSI, the current design of the VB and its location in the linear device. Then, section 3 introduces the simulation setup required to model Magnum-PSI with SOLPS-ITER. The main discussion of results is located in section 4. Two main plasma scenarios are presented: a high flux (HF) and a low flux (LF) scenario. These have peak ion flux values

of  $\sim 1 \times 10^{24} \text{ m}^{-2} \text{ s}^{-1}$  and  $\sim 5 \times 10^{23} \text{ m}^{-2} \text{ s}^{-1}$  at the target, respectively. For these cases, peak temperatures of the plasma are  $\sim 0.8 \text{ eV}$  and  $\sim 1.4 \text{ eV}$  close to the target when no VB is included. Simulations without the VB are used as a reference case to study the effect of the box and the evaporation of Li from the central box. An evaporation temperature of 800 K is used for both plasma scenarios. Finally, conclusions are given in section 5.

## 2. VB geometry and planned experimental setup in Magnum-PSI

The VB experiment currently being designed at DIFFER will be tested in the linear plasma device Magnum-PSI. This machine can recreate the particle and heat fluxes expected at ITER's divertor [15, 16], which makes it an excellent benchmark for testing heat flux dissipation mechanisms.

The current modular design of the VB allows for testing configurations enclosing the target, for an increased containment of neutrals, and in the open configuration for easy access of diagnostics systems to the plasma beam downstream of the VB. Moreover, a liquid metal can be evaporated from inside the box, to generate a cloud that will exchange energy and momentum with the plasma. It is expected that this cloud and the retained neutrals coming from recycling at the target and volumetric recombination will interact with the incoming plasma beam, increasing recombination and reducing the heat flux to the target.

A general scheme of Magnum-PSI is shown in figure 1. The device is divided in three chambers: source (I), beam dump (II) and target (III) chamber. The plasma beam is generated by a cascade-arc source (marked in pink) and it impacts the target (in red), typically tungsten. The main gas injected into the source is typically hydrogen (or deuterium) at a rate of 2–8 slm, depending on the desired conditions. Skimmers (blue) separate the chambers. These skimmers are used to avoid that neutrals coming from the source reach the target chamber, and to allow a pressure in the target chamber independent of the amount of gas injected at the source to generate the plasma. Three sets of pumps, marked as P in the figure, maintain a different pressure in each chamber. An axial magnetic field is generated by a series of superconducting coils located outside the vacuum vessel.

The VB will be located in the target chamber, surrounding the plasma beam. A simplified scheme of the VB in its open configuration can be found in figure 2. The VB is composed of three boxes. The target, located at  $z = 5 \text{ cm}$ , is not enclosed by the VB to allow for easy access with different diagnostics, particularly TS. The central box has the capability to evaporate a liquid metal, typically Li, via an external heater to form a cloud of metal vapour. These metal atoms will then condense in the side boxes, assumed to be at 300 K, although a fraction of them will be able to escape. The VB will not contact directly with the plasma beam, as the minimum diameter of the box hole is larger than the maximum plasma beam diameter achievable in Magnum-PSI, under 5 cm. Thus, any change in the plasma

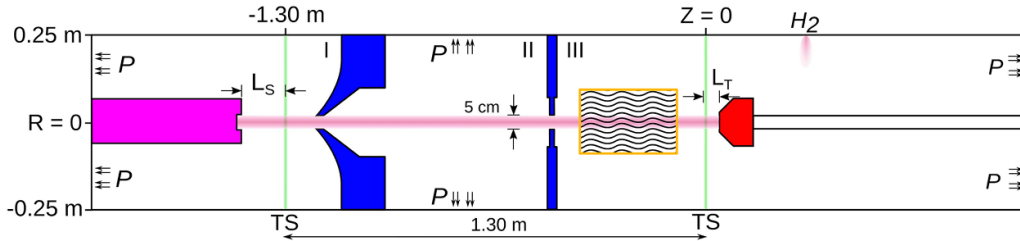


**Figure 1.** Scheme of Magnum-PSI. The skimmers (blue) separate the device in three chambers: source (I), beam dump (II) and target (III). The plasma beam goes from the source (pink) to the target (red). The target can translate along the axial ( $z$ ) direction of the chamber. Vertical green lines indicate the position of Thomson Scattering (TS) measurement system. The pumps (P) remove particles and maintain a low pressure in each chamber. The region in which the VB module will be located is indicated with an orange box.

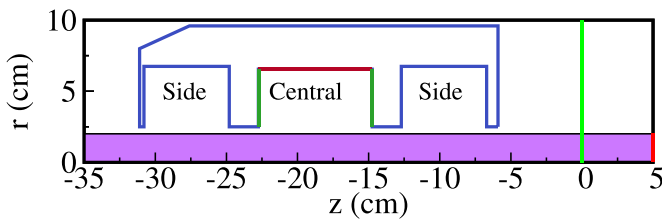


**Figure 2.** Contour of the Vapour Box (blue) in its open configuration as it will be placed in Magnum-PSI. Target is represented in red. Vertical green line represents the TS position. Purple rectangle depicts the plasma beam. Lithium is evaporated from the central box from the surface marked in red. The side limits of the central box (green) are assumed to reflect the evaporated Li. The other surfaces of the VB are cold and will condense the lithium.

beam by the VB will be caused by an increased plasma-neutral interaction. The VB is build in Eirene with additional surfaces, without modifying the mesh, to ease the comparison with the base case that does not include the VB.

### 3. Numerical setup

To test the effectiveness of the design presented in section 2, the SOLPS-ITER [14] code suite is used. Although this software is usually applied to Scrape-off-Layer simulation in tokamak devices, its use in linear devices has been extended in previous years [17–20]. SOLPS-ITER is composed of a CFD plasma module, B2.5, and a kinetic neutral module, Eirene [21, 22]. These two modules are coupled, meaning that B2.5 provides a plasma background for Eirene to compute collisions between plasma and neutrals as well as a recombination source, and Eirene sends to B2.5 sources and sinks of particles, momentum and energy for the plasma species.

To simulate Magnum-PSI with SOLPS-ITER, a rectangular region, assuming an axi-symmetrical geometry, is used to represent the plasma beam. Then, the Eirene grid is extended to cover the full device vessel to properly capture the dynamics of the neutrals outside the plasma region. In the plasma region, the two grids overlap so that information between plasma and neutrals can be communicated. This is shown in figure 3, in which the dark region corresponds to the high density of grid cells in the plasma beam.

At the source boundary condition ( $z = -1.3$  m), a profile of plasma density, temperature and potential is used. The data of density and temperature are usually obtained from TS measurements in Magnum-PSI. The potential profile is unknown, and it is usually calibrated so that the conditions at the TS position near the target match existing experimental data [6]. As this potential profile controls the Ohmic heating applied to the system, plasma temperature is quite sensitive to it.

This unknown profile hinders the predictive capability of SOLPS-ITER regarding Magnum-PSI simulations, as experimental data is always required. Because no experimental data is available for the VB experiment yet, parameters from previous cases successfully simulated are used to generate a High and an LF cases [6].

In addition, the dynamic of neutral particles reflected by the walls of Magnum-PSI has an impact on the neutral distribution and, thus, the plasma properties. Currently, it is assumed that atomic hydrogen has two possible outcomes when interacting with a Magnum-PSI wall: it is either reflected keeping its energy, with a 90% of probability, or it recombines into  $H_2$  and it is reflected by the wall with an energy equivalent to the wall temperature [23]. Molecules are assumed to always be reflected as thermal molecules by the wall. For modelling the interaction of neutral particles with the VB surfaces, the same reflection model as with the walls of Magnum-PSI is assumed. Lithium is always absorbed by the walls of Magnum-PSI and the VB, except for the hot central box from which lithium is evaporated.

To properly simulate Magnum-PSI, the pressure in each chamber must be independently established. This is achieved in SOLPS-ITER by means of a pressure feedback loop. The absorption probability of a boundary surface (corresponding with the location of Magnum-PSI pumps in figure 1), is recalculated during the SOLPS-ITER iterative process with a proportional-integral control loop so that the pressure at a specific position is kept as close as possible to a reference value. The measured pressures for each chamber and the approximated position of these measurements are given to the simulations to achieve the same pressure in each chamber during steady state operation than in Magnum-PSI experiments.

For the plasma impacting the target, a 100% recombination is assumed, being 90% H and the remaining 10%  $H_2$  [23]. An electrically floating target is assumed, meaning that the net

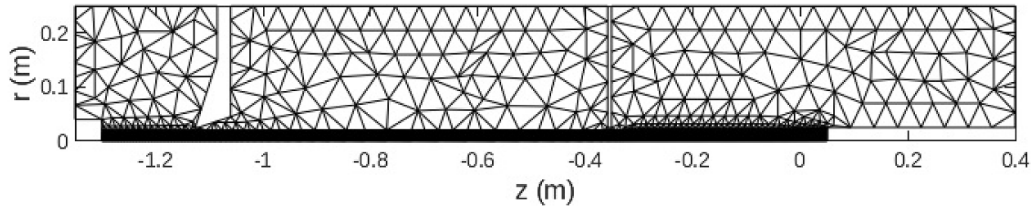


**Figure 3.** Numerical mesh for the simulation of Magnum-PSI without the VB module. The black solid region correspond to the plasma beam, which has a high density number of cells.

**Table 1.** Reactions used by Eirene for atomic and molecular Hydrogen. The type of collision are: charge-exchange (CX), electron impact ionization (EI), elastic collision (EL), dissociation (DS) and recombination (RC). For the neutral-neutral interactions, a BGK approach is employed with the Morse's potential [24].

Collision	Type	Database
$e + H \rightarrow e + H^+ + e$	EI	AMJUEL 2.1.5
$H^+ + H \rightarrow H + H^+$	CX	HYDHEL 3.1.8
$e + H_2 \rightarrow H + H$	DS	AMJUEL 2.2.5 g
$H + H \rightarrow H + H$	EL	BGK
$H + H_2 \rightarrow H + H_2$	EL	BGK
$H_2 + H_2 \rightarrow H_2 + H_2$	EL	BGK
$H^+ + H_2 \rightarrow H + H_2^+$	CX	AMJUEL 3.2.3
$e + H_2^+ \rightarrow H^+ + H^+ + 2e$	DS	AMJUEL 2.2.11
$e + H_2^+ \rightarrow H + H^+ + e$	DS	AMJUEL 2.2.12
$e + H_2^+ \rightarrow H + H$	DS	AMJUEL 2.2.14
$H^+ + H_2 \rightarrow H^+ + H_2$	EL	AMJUEL 0.3 T
$e + H_2 \rightarrow e + H_2^+ + e$	EI	AMJUEL 2.2.9
$e + H_2 \rightarrow H + H^+$	DS	AMJUEL 2.2.10
$H^+ + e \rightarrow H(1 s)$	RC	AMJUEL 2.1.8

current through the target is null, as planned for the Magnum-PSI experiments.

The plasma flux reaching the edge of the beam is automatically recombined and acts as a source of neutral particles in Eirene.

To simulate the interaction between plasma and the neutral hydrogen gas, the set of reactions from table 1 is used in Eirene. Once Eirene has calculated all trajectories for the test particles in the current iteration, it computes the sinks and sources affecting the plasma and passes them to B2.5 to generate a new plasma state. As can be seen from the collision processes employed, interaction between plasma and neutrals exchange energy and momentum but also can create new neutral and ionised particles. The number and intensity of processes inside the VB will determine its effect in the plasma beam.

When lithium is introduced in the simulations, a series of collisional processes need to be included to properly account for the plasma-lithium interaction. These are presented in table 2. The evaporated Li will mostly interact with the plasma beam by means of charge-exchange, elastic collisions and electron impact ionization. The dominant plasma-neutral process will depend on the plasma temperature, as shown in figure 4 For plasma temperatures below 1 eV charge-exchange becomes the main process in the generation of  $Li^+$  while ionization is the dominant term for higher temperatures. Thus, it

**Table 2.** Reactions used by Eirene for atomic lithium. The type of collision are: charge-exchange (CX), electron impact ionization (EI), elastic collision (EL) and recombination (RC). For the neutral-neutral interactions, a BGK approach is employed with the Morse's potential.

Collision	Type	Database
$e + Li \rightarrow e + Li^+ + e$	EI	ADAS SCD96, PLT96
$H + Li^+ \rightarrow H^+ + Li$	CX	ADAS CCD89, PRC86
$H^+ + Li \rightarrow H + Li^+$	CX	[25]
$Li^+ + Li \rightarrow Li + Li^+$	CX	[26]
$H^+ + Li \rightarrow H^+ + Li$	EL	[27]
$Li^+ + H \rightarrow Li^+ + H$	EL	[27]
$H + Li \rightarrow H + Li$	EL	BGK
$H_2 + Li \rightarrow H_2 + Li$	EL	BGK
$Li + Li \rightarrow Li + Li$	EL	BGK
$Li^+ + e \rightarrow Li(1 s)$	RC	ADAS ACD96, PRB96

is important that the VB module is studied in a wide range of Magnum-PSI operational parameters to properly cover all options. Recombination only becomes an important process for very low plasma temperatures, meaning that a large population of ion lithium will exist in the plasma beam after an ionization event or a charge-exchange with a proton. Elastic collisions between heavy species will also play a role in dissipating the energy from the incoming plasma, particularly at low energies.

For the cases presented in this work, lithium is assumed to be evaporated from the central box, the red surface in figure 2, at a constant temperature of 800 K. It is assumed that the evaporation follows the Langmuir evaporation law [28]

$$\Gamma_{\text{evap}} = \frac{p_{Li}}{\sqrt{2\pi m_{Li} kT}} \quad (1)$$

where  $\Gamma_{\text{evap}}$  is the particle flux evaporated in  $m^{-2} s^{-1}$ ,  $m_{Li}$  is the mass of lithium in kg,  $k$  is the Boltzmann constant,  $p_{Li}$  is the vapour pressure of lithium and  $T$  is the temperature in K. The vapour pressure in Pa is defined as [29]

$$\ln(p_{Li}) = 26.89 - \frac{18880}{T} - 0.4942 \ln(T). \quad (2)$$

For a temperature of 800 K the total amount of particles evaporated from the central box lateral surface, red surface in figure 2, is  $\sim 1.15 \times 10^{21} s^{-1}$ .

Only atomic lithium and first ionised state are assumed, meaning that combinations with hydrogen and droplets of Li

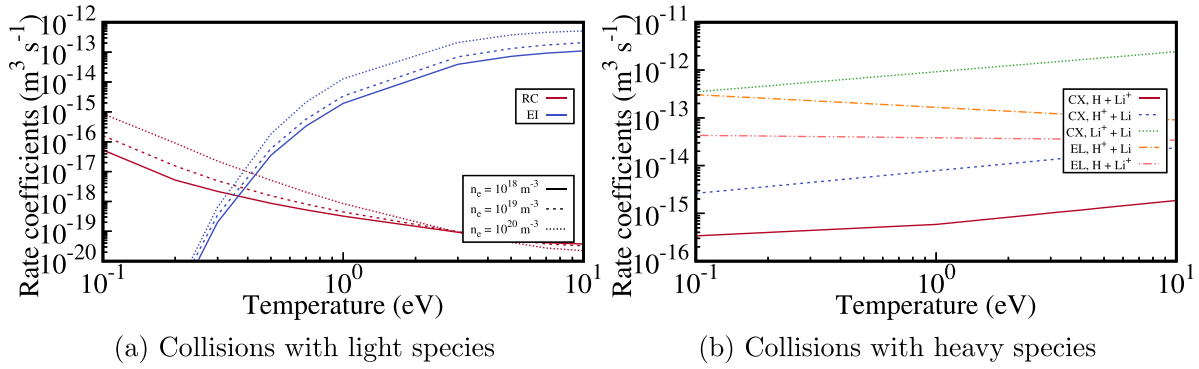


**Figure 4.** Plasma-lithium effective collision rate coefficients for the range of temperatures and densities relevant for Magnum-PSI. Charge-exchange (CX) and elastic collisions (EL) are the dominant processes for  $T_e < 1$  eV while ionization (EI) is the main process at higher temperatures. As recombination (RC) only becomes important for very low plasma temperatures, a significant population of  $\text{Li}^+$  should appear in the plasma.

are neglected. The higher ionised states of lithium, i.e.  $\text{Li}^{2+}$  and  $\text{Li}^{3+}$ , are not accounted for as temperatures in Magnum-PSI are below 5 eV.

Nevertheless, a few *free parameters* still exist in the simulation of Magnum-PSI [6, 20]. These are the electric potential profile at the source boundary condition, mentioned above, and the transport coefficients for B2.5. Normally, these are adjusted to match experimental data [6]. For the cases presented in section 4, scenarios previously modelled will be used as reference cases to study the effect of the VB. After experimental data for certain operational parameters of Magnum-PSI with the VB have been obtained, these free parameters should be adjusted to properly compare simulations and experiments. This will be also a crucial step before simulating the closed configuration of the VB, as the access of diagnostics will be limited and simulations will be crucial to understand the dynamics inside the box. Multiple techniques will be employed to reduce the free-parameters in SOLPS-ITER simulations and provide some validation to the set of A&M processes employed, including TS, calorimetry and lithium deposition on different witness plates located around the VB.

#### 4. Numerical simulations

In this section, a comparison of Magnum-PSI simulations with and without the VB present in an open configuration is discussed. Simulations are used to check the capability of the VB to retain neutrals, increasing the plasma-neutral interaction, as well as the effect on the neutral and plasma distributions when a lithium cloud is generated inside the box by an external heater.

As stated above, Magnum-PSI can operate in a wide range of plasma parameters. Thus, it is important to characterize the VB effect in different plasma regimes. Two plasma scenarios are presented here: a High and an LF case. Both cases run with the same magnetic field  $B = 0.7$  T and the same pressure in the three chambers. Specially relevant is the pressure at the target chamber, which is kept low at 0.3 Pa as no gas puffing is introduced.

The relevant plasma parameters can be found in table 3. In both cases, the electric potential adjusted from previous Magnum-PSI cases simulated with SOLPS-ITER to match temperatures in the target chamber are used. For the HF case, classical transport coefficients obtained using the Braginskii formulation for electron and ion collision time [30] are employed. For the low density case, anomalous transport coefficients are used, adjusting them from similar cases run previously [6]. These transport coefficients are used for the two ion species simulated by B2.5:  $\text{H}^+$  and  $\text{Li}^+$ .

In all cases studied, neutral sources of H and  $\text{H}_2$  in the target chamber come from plasma recycling at the target and volumetric recombination, i.e. without gas puffing. The only source of Li in the simulations is the evaporation from the central box.

##### 4.1. HF scenario

In this plasma scenario, ion and electron densities at the target remain high, usually above  $10^{20} \text{ m}^{-3}$  but temperatures are low, around 1 eV. The atomic hydrogen density at the centre line ( $r = 0$  m) for the three scenarios studied here are presented in figure 5. When the VB is introduced, higher atomic density is achieved in the region in which the box is located. This increase in neutral density in the region of the VB module indicates that its design is successfully retaining neutral particles coming from volumetric recombination and recycling at the target. When lithium is evaporated, a significant increase in atomic density appears. This is a result of the complete recombination of the proton plasma (see figure 9) and the resulting atoms being trapped inside the box until they escape and expand downstream.

These atoms have a probability of being recombined into molecules at the box surfaces, as explained in section 3. The axial distribution of molecular hydrogen at  $r = 0$  m is presented in figure 6. In Magnum-PSI, there are two clear sources of  $\text{H}_2$ : target recycling and wall recombination. When no VB is used, the atoms are recombined in the vessel walls, including recycling at the target. A fraction of these molecules will be pumped but part of it will reach the plasma beam and collide with it. However, the introduction of the VB generates a source

**Table 3.** Relevant parameters for the High and Low Flux cases:  $n_e$  and  $T_e$  are the peak density and temperature at the source,  $D_n$  is the density driven particle diffusion,  $\chi_i$  and  $\chi_e$  are the anomalous ion and electron thermal diffusivity and  $\phi$  is the peak value of the electric potential at the source. These transport coefficients are used for  $H^+$  and  $Li^+$ .

	$n_e(m^{-3})$	$T_e(eV)$	$D_n(m^2 s^{-1})$	$\chi_i(m^2 s^{-1})$	$\chi_e(m^2 s^{-1})$	$\phi(V)$
High Flux	$7.3 \times 10^{20}$	2.08	0.0723	0.8524	0.04	-9.08
Low Flux	$2.4 \times 10^{20}$	2.71	0.03	1.6	1.6	-97.3

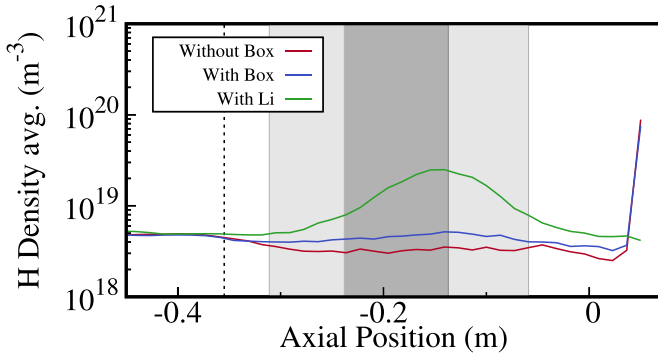


**Figure 5.** Axial distribution of atomic density at the plasma beam axis. The dashed vertical line represents the start of the target chamber in Magnum-PSI. The shadowed rectangles indicate the position of the side and central boxes. The VB has the capability to increase the amount of atoms retained by it, which increases collisionality with the plasma.

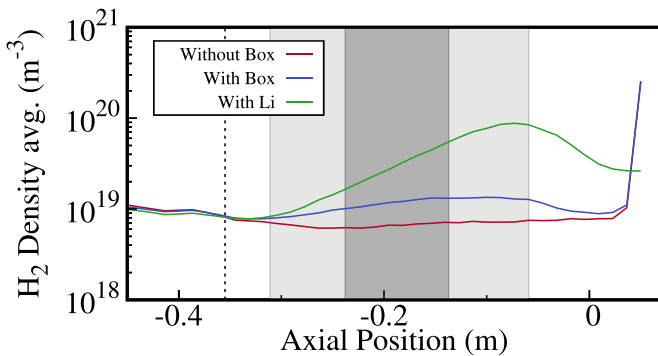


**Figure 6.** Axial distribution of the molecule density at the plasma beam axis. The dashed vertical line represents the start of the target chamber in Magnum-PSI. The shadowed rectangles indicate the position of the side and central boxes. Molecules appearing due to wall recombination of atoms are retained by the box.

of molecules close to the plasma beam due to wall recombination, reducing the probability of them being pumped away from the simulation domain. This explains the increase in molecule density in the region of the VB. These molecules can exchange momentum and energy with the incoming plasma multiple times before leaving the VB.

The Li vapour cloud generated by the VB, presented in figure 7, has the capability to affect the plasma and neutrals in Magnum-PSI by increasing the amount of collisions with the plasma. The largest amount of lithium is found in the central box, from which it is evaporated, and then in the side boxes. In these boxes, the lithium atoms condense as they are at a lower temperature than the central box. Particularly

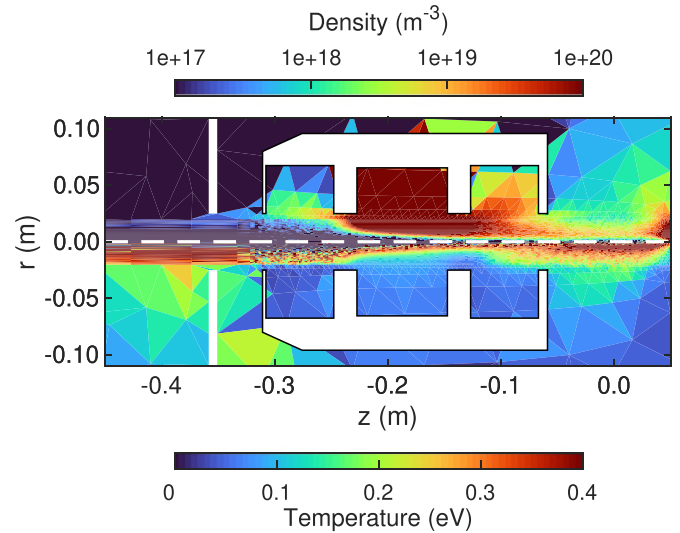
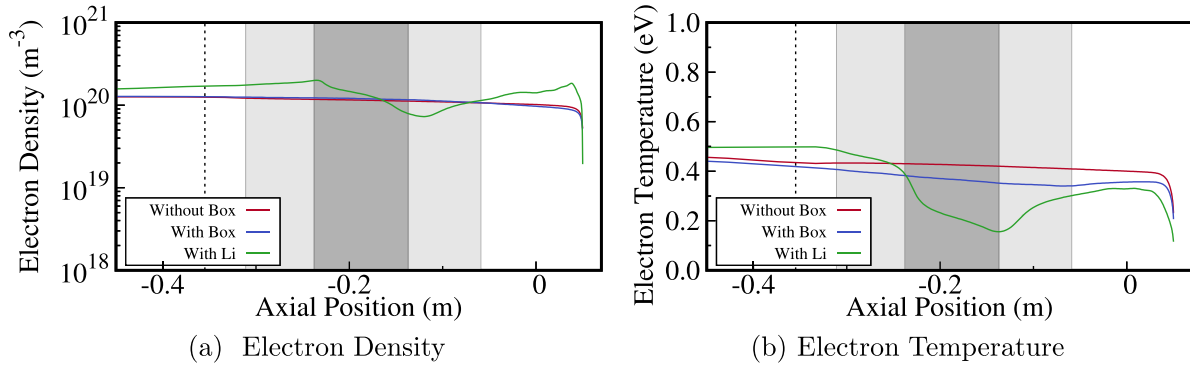


**Figure 7.** Distribution of density (top) and temperature (bottom) for neutral Li. A large amount of Li is retained in the central box while the other two boxes condense it due to their lower wall temperature. Neutral lithium is heated up by collisions with plasma and neutrals to temperatures much larger than the 800 K (0.06 eV) of evaporation.

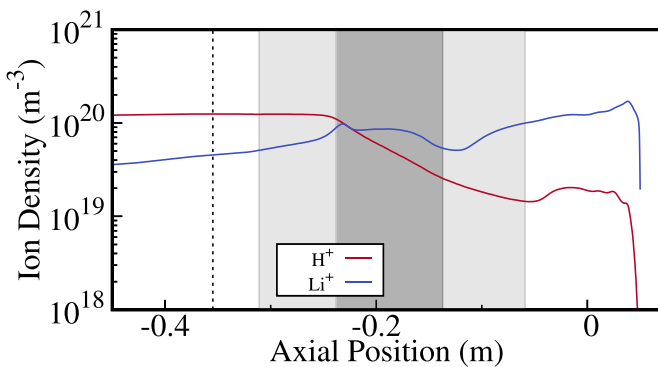
important is the downstream box, which retains most of the lithium (above 40%) as it is being dragged by the plasma beam towards the target, while the upstream box only captures a small amount (around 10%) [13]. However, a fraction of Li escapes downstream towards the target around  $1.2 \times 10^{-2} \Gamma_{\text{evap}}$  ( $1.49 \times 10^{19} \text{ s}^{-1}$ ). A smaller amount in the order of  $5.0 \times 10^{-4} \Gamma_{\text{evap}}$  ( $6.6 \times 10^{17} \text{ s}^{-1}$ ) will escape upstream the VB, being stopped by the skimmer, although part of it ( $7.2 \times 10^{-5} \Gamma_{\text{evap}}$  or  $8.3 \times 10^{16} \text{ s}^{-1}$ ) escapes upstream of the target chamber, reaching the beam dump chamber in Magnum-PSI. During the experiments, a cylindrical witness plate will be located upstream the VB which will collect the escaping lithium. This will be qualitatively compared with the flux obtained from the simulations.

Figure 8 presents the volume average distribution of electron density and temperature along the plasma beam. When the VB is added to the simulations, a slight decrease in electron density and temperature appears. This is a result of the increase in plasma-neutral collisions caused by the retention of particles inside the box. The introduction of lithium has a high impact on the plasma distribution inside the box. A large reduction in electron temperature is found, as the plasma is losing energy by the interaction with the lithium cloud. At this low electron temperature, the main plasma-neutral process interaction is charge-exchange with  $H^+$ . Thus, a plasma proton





**Figure 8.** Volume average electron density (left) and temperature (right) in the region of the VB for the High Flux scenario. The box without lithium produces a lower plasma temperature overall, although temperature increases. When lithium is evaporated, a significant cooling and recombination effect of the plasma appears.



**Figure 9.**  $\text{H}^+$  and  $\text{Li}^+$  volume averaged density in the region of the VB for the High Flux scenario when lithium is evaporated. Lithium ions become the dominant species in the plasma beam inside the central box. A small portion of lithium ions is transported upstream.

will become a hydrogen atom, which interacts with the walls of the VB, until it recombines into  $\text{H}_2$  and escapes downstream (see figure 6). Moreover, a reduction in the electron density appears due to the recombination of lithium ion at low electron temperatures (see figure 4(a)), meaning that the plasma downstream of the box has lower density than upstream.

The distribution of ions for the different species studied here ( $\text{H}^+$  and  $\text{Li}^+$ ) is presented in figure 9 for the case in which lithium is evaporated. An inflexion point in the ion density appears, around  $z = -0.2$  m, just at the start of the central box, in which lithium ions become the dominant species of the plasma as protons are recombined into atomic hydrogen. This occurs by two main processes: charge-exchange between protons and lithium atoms and electron impact ionization and excitation of Li. Due to the lower ionization potential of Li with respect to H electrons have a larger probability to pass from lithium to hydrogen, as well as they are easier to ionize up to the first level. During this process, the plasma losses a large fraction of energy. A very small portion of lithium ions is transported towards the source through the plasma edges, but this is orders of magnitude below the proton density and should not present an issue during the experiments as long as the duration of the shots is short enough that the amount of neutral and ion lithium travelling upstream does

not accumulate in important regions of Magnum-PSI, e.g. the viewports and the plasma source.

The VB has the capability of reducing the particle and heat fluxes towards the target as it is depicted in figure 10. The retention of neutrals resulting from the box geometry slightly reduces the heat flux towards the target by  $\sim 0.2 \text{ MW m}^{-2}$  at the beam peak, a reduction of  $\sim 21\%$ . This is achieved without any additional gas puffing or introducing new particles into the domain. The lithium cloud has a clear effect in reducing the heat flux at the peak by  $\sim 0.7 \text{ MW m}^{-2}$ ,  $\sim 80\%$ , and the ion particle flux by a factor larger than 2. Moreover, the influx of protons to the target is completely substituted by lithium when a cloud is generated inside the VB.

#### 4.2. LF scenario

When Magnum-PSI operates at a lower density, plasma temperatures are higher. This has an impact in the relevant plasma-neutral interactions [7], and thus, it is expected a different behaviour of the VB than in the previous section. Moreover, lower densities result in fewer recycled neutrals, which could translate to a reduction in the VB efficiency.

Figure 11 depicts the density of atomic hydrogen for the three scenarios studied here. The VB by itself is also capable of slightly increasing the neutral density as in the HF case. In addition, when Li is evaporated from the central box, the same effect as in the HF case appears, meaning that for this scenario the lithium cloud is also capable of mitigating the incoming plasma, increasing the amount of neutral lithium mostly at the central box, where lithium-proton interactions largely take place. The same increase of density is found for molecular hydrogen, as shown in figure 12, meaning that atoms are being recycled at the VB walls and these molecules are also retained by the box. When Li is evaporated from the central box, hydrogen in the plasma is completely recombined, creating a rise in atomic and molecular densities inside the box. Thus, similar effects as in the HF scenario appear, despite the lower plasma and neutral densities in this situation. As in the HF case, most of the Li condenses in the downstream box and a fraction of the evaporated lithium escapes upstream ( $1.6 \times 10^{18} \text{ s}^{-1}$ ) and downstream ( $2.9 \times 10^{19} \text{ s}^{-1}$ ),

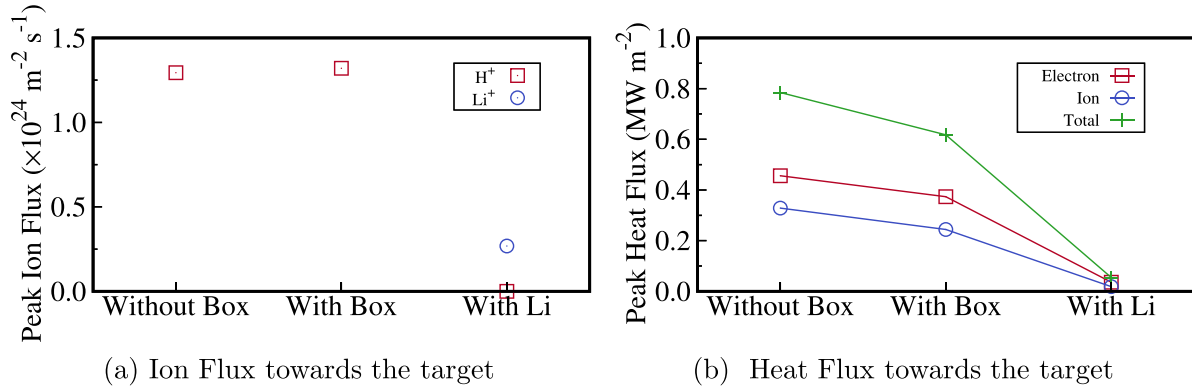


**Figure 10.** Ion particle flux (left) and heat fluxes (right) at the centre of the plasma beam (peak) towards the target for the three cases presented here for the HF scenario. Neutral fluxes towards the target are not depicted as they are orders of magnitude below ion fluxes. The introduction of the VB results in a slight reduction in the peak heat flux. The lithium cloud inside the box has a clear effect on reducing fluxes towards the target.

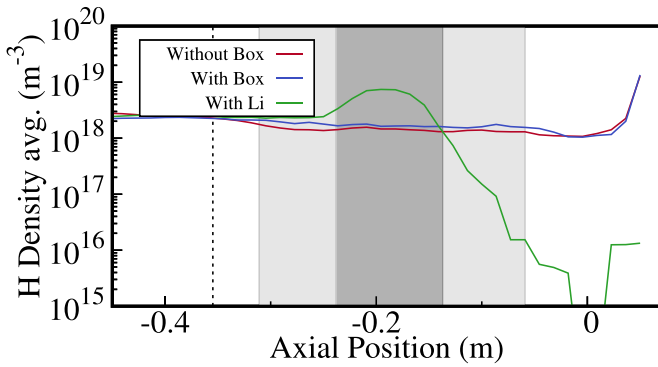


**Figure 11.** Distribution of atomic hydrogen density for the Low Flux case in three scenarios. The dashed vertical line represents the start of the target chamber in Magnum-PSI. The shadowed rectangles indicate the position of the side and central boxes. The VB has the capability to retain atoms in the region of effect. The addition of Li strongly increases recombination of protons.

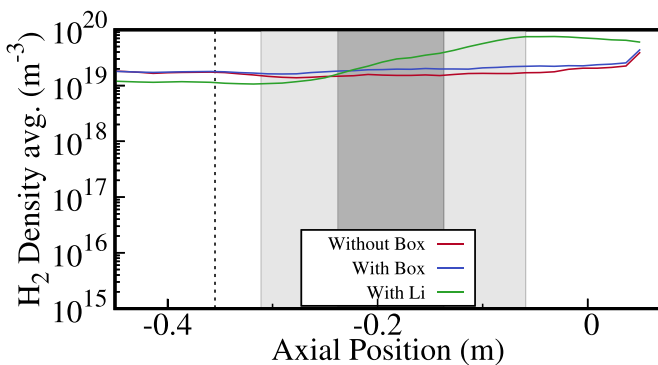


**Figure 12.** Distribution of  $\text{H}_2$  density at the plasma beam axis. The dashed vertical line represents the start of the target chamber in Magnum-PSI. The shadowed rectangles indicate the position of the side and central boxes. The VB successfully retains molecules from surface recombination.

although these amounts are a small fraction ( $1.4 \times 10^{-3}$  and  $2.5 \times 10^{-2}$ , respectively) of  $\Gamma_{\text{evap}}$ . Part of the upstream flux of neutral lithium ( $7.3 \times 10^{-4} \Gamma_{\text{evap}}$  or  $8.3 \times 10^{17} \text{ s}^{-1}$ ) escapes the

target chamber, reaching the beam dump chamber. However, this very small fraction of neutral lithium is not expected to affect the operation of Magnum-PSI during the experiments.

Figure 13 shows the volume average values of electron density and temperature for the LF scenario in the three cases studied: without the box, with the VB and with evaporation of Li. The VB results in a reduction of electron temperature, slightly reducing the density. The evaporation of lithium from the central box has a large cooling effect in the plasma beam, as depicted in figure 13(b), but recombination of lithium is neglectable (see figure 4), meaning that electron density increases due to secondary electrons from lithium ionization. In this scenario the lithium cloud is also capable of mitigating the plasma beam. As shown in figure 14 in a LF situation lithium also becomes the dominant ion species inside and from downstream the VB module. So, the high temperature low density upstream hydrogen plasma becomes a low temperature low density lithium plasma due to the evaporation inside the VB.

As in the HF case, the VB has a significant effect on the fluxes towards the target, depicted in figure 15. The box by itself reduces both, the particle and heat fluxes, by simply retaining neutral particles coming from volumetric recombination and target recycling. When Li is evaporated, the resulting cloud has the capability of reducing heat flux by a factor  $\sim 0.6 \text{ MW m}^{-2}$  with respect to the case without the VB, a reduction of  $\sim 75\%$ . A decrease in particle flux is still achieved, as shown in figure 15(a), meaning that a fraction of lithium escapes downstream the VB. However, this fraction is only  $\sim 3\%$  of the evaporation flux and mostly ends up being deposited at the target. Thus, the side boxes are responsible of retaining most of the neutral lithium being evaporated.

Once again, simulations show that the VB is an excellent device to mitigate the plasma passing through the VB, specially when a lithium cloud is generated. Although these simulations will need to be verified with future experimental data, the analysis in disparate plasma scenarios presented here shows that the principle of operation of the VB is valid in the wide regime of operation of which Magnum-PSI is capable to operate.

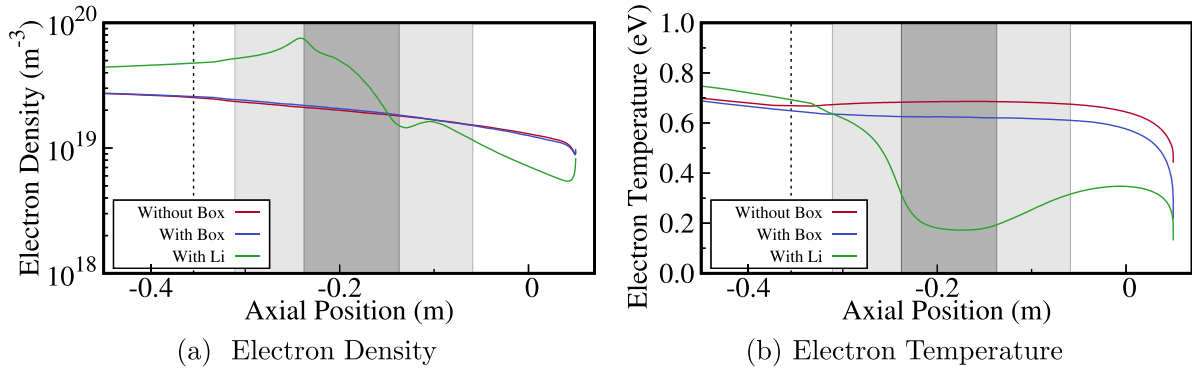


**Figure 13.** Volume average electron density (left) and temperature (right) in the region of the VB for the Low Flux scenario. The evaporation of lithium has a huge impact in reducing the plasma temperature.

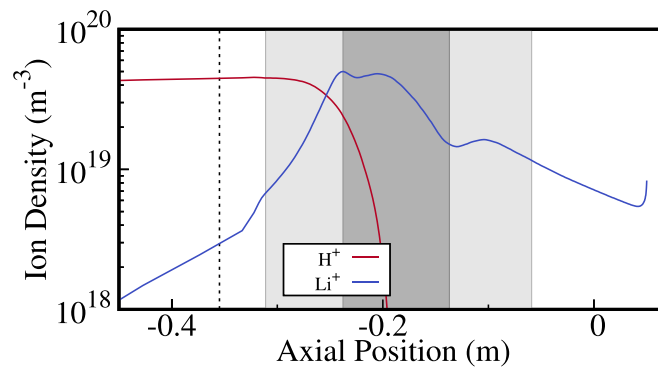


**Figure 14.** Distribution of  $H^+$  and  $Li^+$  volume average density for the Low Flux scenario.

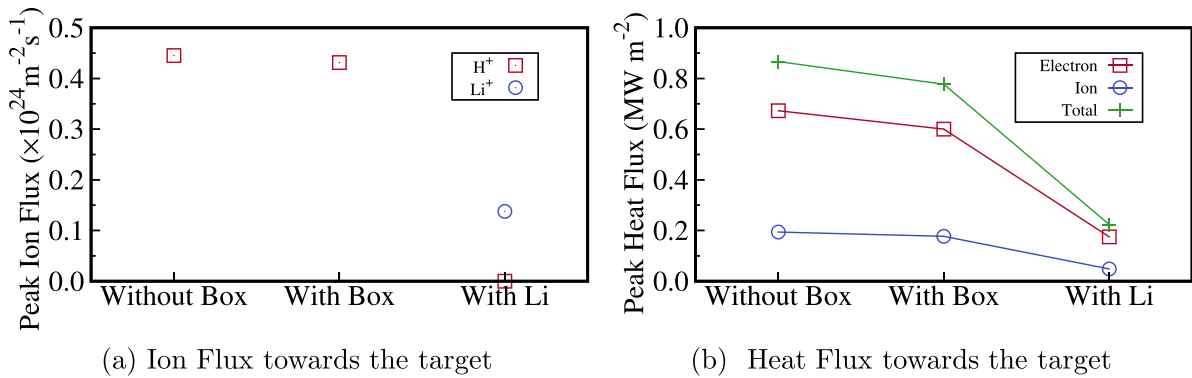


**Figure 15.** Ion particle flux (left) and heat fluxes (right) at the centre of the plasma beam (peak) towards the target for the three cases presented here for the HF scenario. The introduction of the VB results in a slight reduction in the peak heat flux. The lithium cloud inside the box has a clear effect on reducing fluxes towards the target.

### 5. Conclusions

An VB is a concept proposed in the past [10–12] to reduce the heat flux towards divertors in fusion devices. This work focuses in studying the design proposed to be tested in Magnum-PSI in its open configuration in a High and LF plasma scenarios. The open configuration will be used for the first experiments to have an easy access of experimental diagnostics, particularly TS, before and after the VB. This will allow to fully characterize the VB effect before a configuration enclosing the target is tested.

Simulations presented here prove that the VB has the capability to aid in mitigating the plasma beam fluxes towards the target, even in its open configuration, in the two scenarios presented. Atoms deriving from recombination and recycling are trapped by the box, which may then recombine into molecules when colliding with the VB walls. These particles also interact with the plasma beam until they escape the box, reducing the particle and heat fluxes.

Evaporation of a small amount of lithium from the central box has a cooling effect in the plasma beam, resulting in lithium becoming the dominant species due to CX and

electron impact ionization/excitation of Li atoms as the ionization potential of lithium is lower than for hydrogen. The relevant collisional process depends on the plasma temperature, being charge-exchange the dominant process for  $T_e < 1$  eV. Recombination only plays a significant role at very low electron temperatures. This means that the high energy incoming hydrogen plasma is substituted by a low energy lithium plasma in which proton density is orders of magnitude lower.

Simulations estimate that the amounts of lithium particles escaping upstream and downstream from the VB module are three and two orders of magnitude below the evaporated amount, respectively. Thus, the side boxes are able to retain most of the lithium escaping the central box. Still, a small fraction of neutral lithium is dragged towards the target by the plasma beam. An additional fraction of lithium is being ionised and dragged towards the target. As more lithium is being dragged towards the target, the downstream side box is the one retaining most of the lithium. Another smaller fraction of Li and  $\text{Li}^+$  moves upstream the VB, but it should not be an issue for the operation of Magnum-PSI during experiments as it is orders of magnitude below the evaporated amount. These fluxes should be taken into account to avoid over-saturating Magnum-PSI walls, pumps and viewing ports with lithium during the experiments. Translating these fluxes to a tokamak is not easy, as geometrical factors play an extremely important role. However, taking into account that simulations of the VB module in Magnum-PSI show how most of the lithium is condensed in the side boxes or transported downstream the VB, this could indicate that core contamination may not become a relevant issue for an VB in a divertor. Nevertheless, this should be addressed with simulations for specific designs of the VB.

Experimental validation of these simulations is still required to deal with the free parameters necessary for the simulation of Magnum-PSI with SOLPS-ITER and to validate the A&M processes employed when lithium is incorporated into the simulations. This will also increase the reliability of simulations when the case of an VB module enclosing the target is analysed. It is expected that this closed configuration will have even a higher effect in reducing fluxes towards the target. This could be a method to reduce significantly the heat fluxes towards the divertor without contaminating the core in fusion reactors once that this design is extrapolated to a toroidal geometry.

### Data availability statement

The data that support the findings of this study are openly available at the following URL/DOI: <https://zenodo.org/record/7737149>.

### Acknowledgments

This work has been carried out within the framework of the EUROfusion Consortium, funded by the European Union via the Euratom Research and Training Programme (Grant Agreement No. 101052200 – EUROfusion). Views and opinions

expressed are however those of the author(s) only and do not necessarily reflect those of the European Union or the European Commission. Neither the European Union nor the European Commission can be held responsible for them. The general development of EIRENE goes within EUROfusion E-TASC TSVV-5 project. This work was carried out on the Dutch national e-infrastructure with the support of SURF Cooperative and the EUROfusion High Performance Computer Marconi-Fusion hosted at Cineca (Bologna, Italy). This work is part of the research programme ‘The Leidenfrost divertor: a lithium vapour shield for extreme heat loads to fusion reactor walls’ with project number VI.Vidi.198.018, which is (partly) financed by NWO. The authors would like to thank one of the referees for identifying a crucial error in the first version of this manuscript regarding the relevant collision process between hydrogen and lithium.

### ORCID iDs

J Gonzalez  <https://orcid.org/0000-0001-7905-5001>  
 E Westerhof  <https://orcid.org/0000-0002-0749-9399>  
 T W Morgan  <https://orcid.org/0000-0002-5066-015X>

### References

- [1] Kuang A Q *et al* 2020 Divertor heat flux challenge and mitigation in SPARC *J. Plasma Phys.* **86** 865860505
- [2] Kukushkin A S, Pacher H D, Kotov V, Pacher G W and Reiter D 2011 Finalizing the ITER divertor design: the key role of SOLPS modeling *Fusion Eng. Des.* **86** 2865–73
- [3] Im K, Kwon S and Sung Park J S 2016 A preliminary development of the K-DEMO divertor concept *IEEE Trans. Plasma Sci.* **44** 2493–501
- [4] Wischmeier M *et al* 2009 Current understanding of divertor detachment: experiments and modelling *J. Nucl. Mater.* **390** 250–4
- [5] Soukhanovskii V A *et al* 2007 Divertor heat flux reduction and detachment experiments in NSTX *J. Nucl. Mater.* **363** 432–6
- [6] Chandra R, De Blank H J, Diomede P, Van Eck H J N, Van Der Meiden H J, Morgan T W, Vernimmen J W M and Westerhof E 2021 B2. 5-Eunomia simulations of Magnum-PSI detachment experiments: I. Quantitative comparisons with experimental measurements *Plasma Phys. Control. Fusion* **63** 095006
- [7] Chandra R, de Blank H J, Diomede P and Westerhof E 2021 B2. 5-Eunomia simulations of Magnum-PSI detachment experiments: II. Collisional processes and their relevance *Plasma Phys. Control. Fusion* **64** 015001
- [8] Nygren R E *et al* 2004 A fusion reactor design with a liquid first wall and divertor *Fusion Eng. Des.* **72** 181–221
- [9] Nagayama Y 2009 Liquid lithium divertor system for fusion reactor *Fusion Eng. Des.* **84** 1380–3
- [10] Goldston R, Emdee E, Jaworski M, Schwartz J, Rognlien T and Rensink M 2019 Development of a lithium vapour box divertor for controlled plasma detachment *Nucl. Fusion IAEA FEC* 2018
- [11] Romano F, Rindt P, Scholten J, Hayashi Y and Morgan T W 2021 Effect of lithium vapour shielding on hydrogen plasma parameters *Phys. Scr.* **96** 125626
- [12] Schwartz J A, Emdee E D, James Goldston R J and Jaworski M A 2019 Physics design for a lithium vapor box divertor experiment on magnum PSI *Nucl. Mater. Energy* **18** 350–5

- [13] Schwartz J A and Goldston R J 2021 Developments on two lithium vapor-box linear test-stand experiments *Nucl. Mater. Energy* **26** 100901
- [14] Wiesen S et al 2015 The new SOLPS-ITER code package *J. Nucl. Mater.* **463** 480–4
- [15] De Temmerman G, Van Den Berg M A, Scholten J, Lof A, Van Der Meiden H J, Van Eck H J N, Morgan T W, De Kruijf T M, Zeijlmans Van Emmichoven P A and Zielinski J J 2013 High heat flux capabilities of the Magnum-PSI linear plasma device *Fusion Eng. Des.* **88** 483–7
- [16] van Eck H J N et al 2019 High-fluence and high-flux performance characteristics of the superconducting Magnum-PSI linear plasma facility *Fusion Eng. Des.* **142** 26–32
- [17] Baeva M, Goedheer W J, Lopes Cardozo N J and Reiter D 2007 B2-EIRENE simulation of plasma and neutrals in MAGNUM-PSI *J. Nucl. Mater.* **363** 330–4
- [18] Rapp J, Owen L W, Canik J, Lore J D, Caneses J F, Kaffle N, Ray H and Showers M 2019 Radial transport modeling of high density deuterium plasmas in proto-MPEX with the B2. 5-Eirene code *Phys. Plasmas* **26** 042513
- [19] Sala M, Tonello E, Uccello A, Bonnin X, Ricci D, Dellasega D, Granucci G and Passoni M 2020 Simulations of Argon plasmas in the linear plasma device GyM with the SOLPS-ITER code *Plasma Phys. Control. Fusion* **62** 055005
- [20] Gonzalez J, Chandra R, de Blank H J and Westerhof E 2022 Comparison between SOLPS-ITER and B2. 5-Eunomia for simulating Magnum-PSI *Plasma Phys. Control. Fusion* **64** 105019
- [21] Reiter D, Baelmans M and Börner P 2005 The EIRENE and B2-EIRENE codes *Fusion Sci. Technol.* **47** 172–86
- [22] Borodin D V et al 2021 Fluid, kinetic and hybrid approaches for neutral and trace ion edge transport modelling in fusion devices *Nucl. Fusion* **62** 086051
- [23] Wieggers R C, Coster D P, Groen P W C, De Blank H J and Goedheer W J 2013 B2. 5-Eunomia simulations of Pilot-PSI plasmas *J. Nucl. Mater.* **438** S643–6
- [24] Bachmann P and Reiter D 1995 Kinetic description of elastic processes in hydrogen-helium plasmas *Contrib. Plasma Phys.* **35** 45–100
- [25] Braams B J and Chung H-K 2015 Light element atom, molecule and radical behaviour in the divertor and edge plasma regions *J. Phys.: Conf. Ser.* **576** 011001
- [26] Marenkov E D, Pshenov A A and Kukushkin A S 2020 Shielding of liquid metal targets in plasma of linear devices *Phys. Plasmas* **27** 062514
- [27] Krstić P S and Robert Schultz D R 2009 Elastic and related transport cross sections for singly charged ion–atom scattering of light metals (Li, Be, B) and hydrogen *J. Phys. B: At. Mol. Opt. Phys.* **42** 065207
- [28] Langmuir I 1917 The condensation and evaporation of gas molecules *Proc. Natl Acad. Sci. USA* **3** 141
- [29] Honig R E 1969 Vapor pressure data for the solid and liquid elements *RCA Rev.* **30** 285–305
- [30] Braginskii S I 1965 Transport processes in a plasma *Rev. Plasma Phys.* **1** 205